

INTERACTION OF LASER RADIATION WITH MATTER https://doi.org/10.1070/QEL17426

Destruction of absorbing metal films during laser printing with gel microdroplets

V.S. Zhigarkov, N.V. Minaev, V.I. Yusupov

Abstract. **The degree of destruction and evaporation of metal films (Au and Ti, thickness ~50 nm) with a gel layer during laser transfer of small volumes of a gel substrate is estimated depending on the laser fluence value. The dynamics of these processes for dry films and films with a gel layer at fluences close to threshold values is investigated using a probe beam of a He–Ne laser. It is shown that the presence of a gel leads to an increase in the ablation threshold, but the time during which the process of structural changes in the film material is completed does not change significantly. The results obtained can be used to improve the laser bioprinting technology.**

Keywords: *laser printing, gel microdroplets, Au and Ti metal films, ablation.*

1. Introduction

The technology of laser-induced forward transfer of matter, or laser printing [1–10], is widely used in biomedicine. One of the successfully developed areas is the method of laser engineering of microbial systems (LEMS) [3, 11] for the isolation of microorganisms uncultivated and difficult to cultivate [12, 13]. The method is based on the transfer of small volumes of a gel substrate with living cells and microorganisms due to thermal cavitation caused by the absorption of a nanosecond laser pulse by a thin metal layer.

In laser printing on a donor plate (a glass plate with a thin absorbing metal layer of gold, titanium, chromium, etc.), a layer of a gel substrate is applied, which may contain biomolecules [2, 3], living cells [1], and microorganisms [4, 11–13]. The impact of focused pulsed laser radiation leads to local heating of the metal layer and the emergence of a rapidly expanding cavitation bubble [11], as a result, a small volume of gel containing a small number of living cells or microorganisms is transferred to the receiving media. However, due to strong heating, the effect of focused radiation leads to the destruction and evaporation of the metal film, as well as to the ejection of metal particles together with the gel substrate [11, 14]. These factors can affect the transferred living systems; therefore, to improve the technology of laser printing, it is necessary to select the optimal regimes of laser exposure. To this end, it is necessary to consider the processes induced by the absorption of a nanosecond laser pulse with an appropriate time resolution, paying special attention to the dynamics of changes in the morphology, melting, and destruction of the absorbing film exposed to laser radiation with fluence (surface energy density) both above and below the ablation threshold. Studies must be carried out both with a gel layer on a metal film (conditions for laser printing with gel microdroplets) and without it.

This problem can be efficiently solved by studying the dynamics of the reflectivity of a thin absorbing metal layer using probe laser radiation [15–19] and comparing the results with optical and electronic micrographs of destroyed and modified areas.

The aim of this work is to study the dynamics of changes in the morphology and destruction of absorbing Au and Ti films of the donor substrate under nanosecond laser irradiation with fluences both above and below the ablation threshold under the conditions of gel microdroplets transfer.

2. Description of the experiment

The experiment is schematically illustrated in Fig.1. The source of radiation with λ= 1064 nm was a YLPM-1-1x120-50-M ytterbium fibre pulsed laser (IPG IRE Polyus, Russia) with a tunable pulse duration (τ = 1–120 ns) and pulse energy E_p = 2–900 μJ (beam quality parameter M^2 < 1.34). The laser pulse energy was calibrated using a thermal sensor S310C (Thorlabs, USA). To control the radiation, a two-mir-

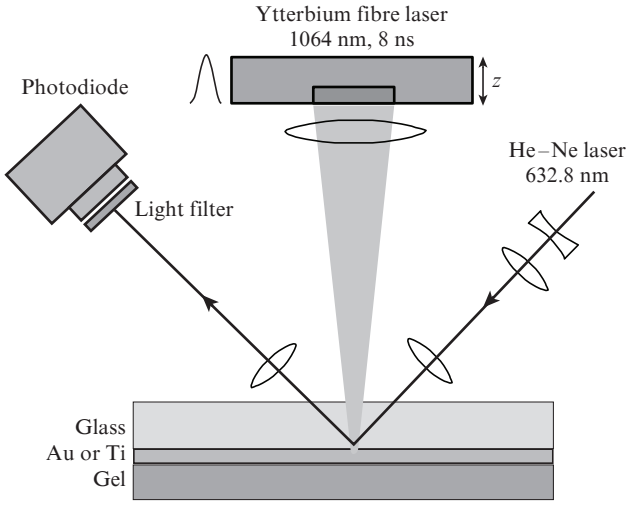

Figure 1. Schematic of the experiment.

V.S. Zhigarkov, N.V. Minaev, V.I. Yusupov Institute of Photonic Technologies, Federal Research Centre 'Crystallography and Photonics', Russian Academy of Sciences, ul. Pionerskaya 2, 108840 Troitsk, Moscow, Russia; vzhigarkov@gmail.com

Received 27 August 2020
Kvantovaya Elektronika **50** (12) 1134–1139 (2020)
Translated by V.L. Derbov

ror galvanic scanning head LscanH-10-1064 (Ateko-TM, Russia) with an SL-1064-110-160 objective lens (Ronar-Smith, Singapore) having a focal length of 160 mm (spot diameter at focus ~30 μm) was used. The focus position relative to the studied object was adjusted using a motorised vertical translator. The pulsed radiation acted on Ti and Au metal films on glass substrates. The thickness of the films was ~50 nm. In a number of experiments, a layer of gel (2% aqueous solution of hyaluronic acid) ~200 μm thick was deposited on the metal film.

A beam of a single-frequency He–Ne laser L02/2 (SIOS, Germany) with high frequency stability ($\lambda = 632.8$ nm, output power 3 mW) was directed (at an angle of ~40° to the normal to the surface of the glass substrate) onto the site of pulsed laser action by means of a system of mirrors, lenses and microscrews, and a beam expander. The laser radiation was focused on the metal layer into a spot with a diameter of ~30 μm. Focus control was carried out using an XCAM1080PHB/PHD/PHE digital camera (ToupTek Photonics, China) with a long-focus lens and an operating field of 4×6 mm. The laser radiation consists of two mutually perpendicular linearly polarised modes. In the experiment, p-polarised radiation was used, which was obtained using a system including a polariser, an analyser, and a half-wave plate.

The reflected He–Ne laser beam was focused on the active region surface of an ODA04A photodetector (Avesta, Russia) equipped with an amplifier. The diameter of the photodetector active region was 0.4 mm, its spectral range was 320–1000 nm, the bandwidth was from 0 to 500 MHz, and the time constant was about 2 ns. A narrow-band interference light filter with a passband of 625–640 nm was placed in front of the photodetector. The He–Ne laser signal was recorded using a GDS-72304 digital four-channel oscilloscope (GW Instek, Taiwan) with a frequency band of 0–300 MHz. The signal recording was synchronised with a pulse acting on a metal film using an additional OD-007B photodetector (Avesta, Russia) with a spectral range of 900–1700 nm, a bandwidth of up to 1700 MHz, and a time constant of 500 ps. This photodetector was placed under the test sample, on the axis of the pulsed laser radiation source. After laser exposure, the samples were examined using a PHENOM ProX scanning electron microscope (Phenom World, the Netherlands) and an HRM-300 Series optical 3D microscope (Huvitz, Korea). The structure of a titanium film on a glass substrate was analysed using a MiniFlex 600 X-ray diffractometer (Rigaku, Japan).

3. Results of measurements and discussion

It is known that when a short laser pulse with a sufficiently high intensity acts on a metal surface, an intense heating of the exposed region occurs due to the partial absorption of radiation [14, 20]. As a result, when the ablation threshold is exceeded, the material evaporates in the centre and melts at the edges of the irradiated area, and the accompanying hydrodynamic effects contribute to the partial or complete removal of the material from the laser exposure zone [21, 22].

From the obtained dependences of the diameters of holes in Ti and Au metal films on the pulse energy, assuming a Gaussian intensity distribution in the laser beam cross section, we can relate the measured diameter of holes $2r_d$ in the Au and Ti films with the threshold value of the laser fluence F_{th} [23]:

$$F_{th} = F\exp\left(-\frac{r_d^2}{2r_f^2}\right),$$

where F is the laser pulse fluence; r_d is the measured radius of the hole in the film; and r_f is the radius of the focal spot. Transforming the above expression, we obtain

$$r_d^2 = 2r_f^2 \ln\left(\frac{F}{F_{th}}\right).$$

Figure 2 shows the dependences of the square of the diameters of the holes obtained in the Au and Ti films on the value of the logarithm of the laser fluence. The corresponding optical micrographs are also shown here. The obtained dependences were used to estimate the threshold fluence values F_{th} for dry (without gel) films: for gold $F_{th} \approx 180$ mJ cm^{-2}, for titanium $F_{th} \approx 60$ mJ cm^{-2}.

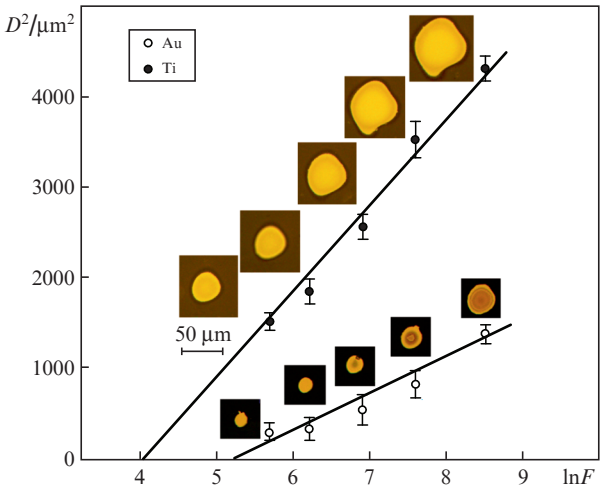

Figure 2. (Colour online) Dependences of the square of the diameters of the holes obtained in Au and Ti films without a gel layer on the natural logarithm of the laser fluence (in mJ cm^{-2}) and their linear approximations. The insets show the corresponding optical micrographs with illumination through film.

The presence of a gel layer on the absorbing metal layer of the donor substrate increases the ablation threshold. As can be seen from the example of a titanium film (Fig. 3), the formation of a hole in it occurs at higher fluence values as compared to a dry sample. Such a result is quite expected, since the presence of the gel leads to an additional outflow of heat from the metal film and a decrease in its heating. Note that there is no visible destruction of the film in the region of laser action at the minimum fluence value (27 mJ cm^{-2}) in the presence of gel (Fig. 3b). In the case of a dry film, with the same fluence, the presence of cracks and micron-size holes can be seen in the affected spot. Similar cracks are also observed in the peripheral region of the spot at high fluence values.

Figure 4 shows SEM images and a topographic picture of the surfaces of Ti and Au films at the threshold values of the laser fluence. In the case of a gold film, in the centre of the laser spot its strong deformation in the region of ~15 μm and a slight destruction with the formation of a rupture of ~ μm are observed. Probably, the gold melting temperature was reached in the centre of the spot, and the film was deformed as a result of its shock-like detachment from the substrate. It is also worth noting that an increase in the fluence to 210 mJ cm^{-2} leads to the formation of a hole in the gold film

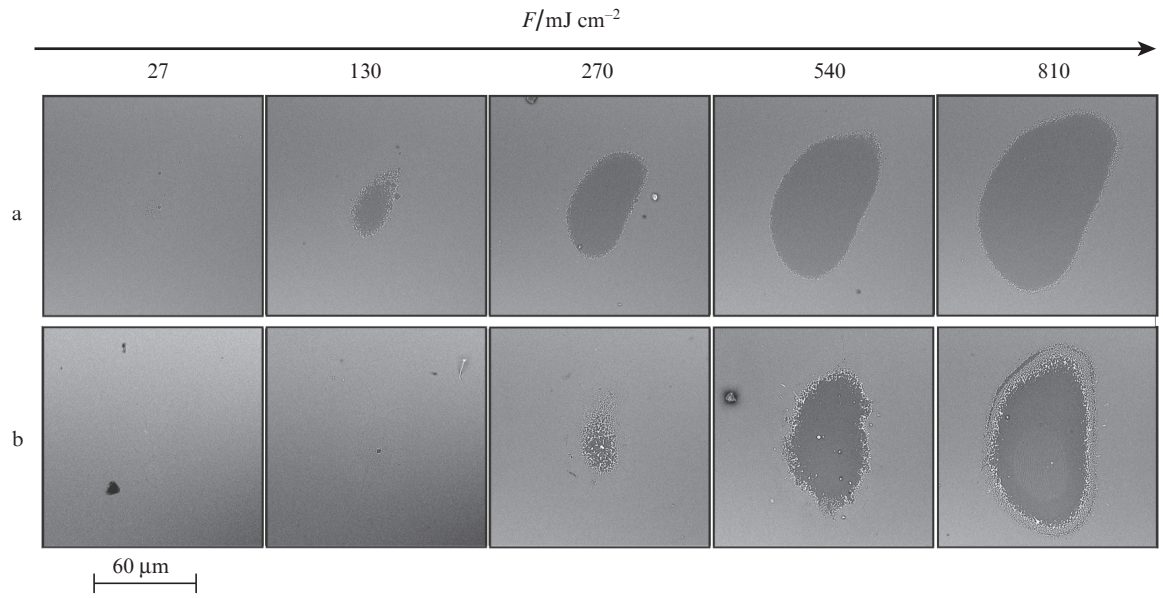

Figure 3. SEM images of the titanium film surface (a) without gel and (b) with gel at various fluence values.

with the appearance of several radial ruptures (due to the extremely weak adhesion of the Au film to the glass substrate) and peeling of the petals.

SEM images of the surface of the titanium film (Fig. 4) show that in the process of thermal laser exposure, there occurred a change in the film morphology, characterised by the formation of numerous cracks having an irregular structure. At the same time, the topographic picture of the surface did not reveal significant height differences. The adhesion of the titanium film to the glass substrate is very high; therefore, the pulse pressure in this case was insufficient to detach the film from the substrate. We believe that the observed effect of cracking occurs due to different values of the coefficients of thermal expansion of glass and metal.

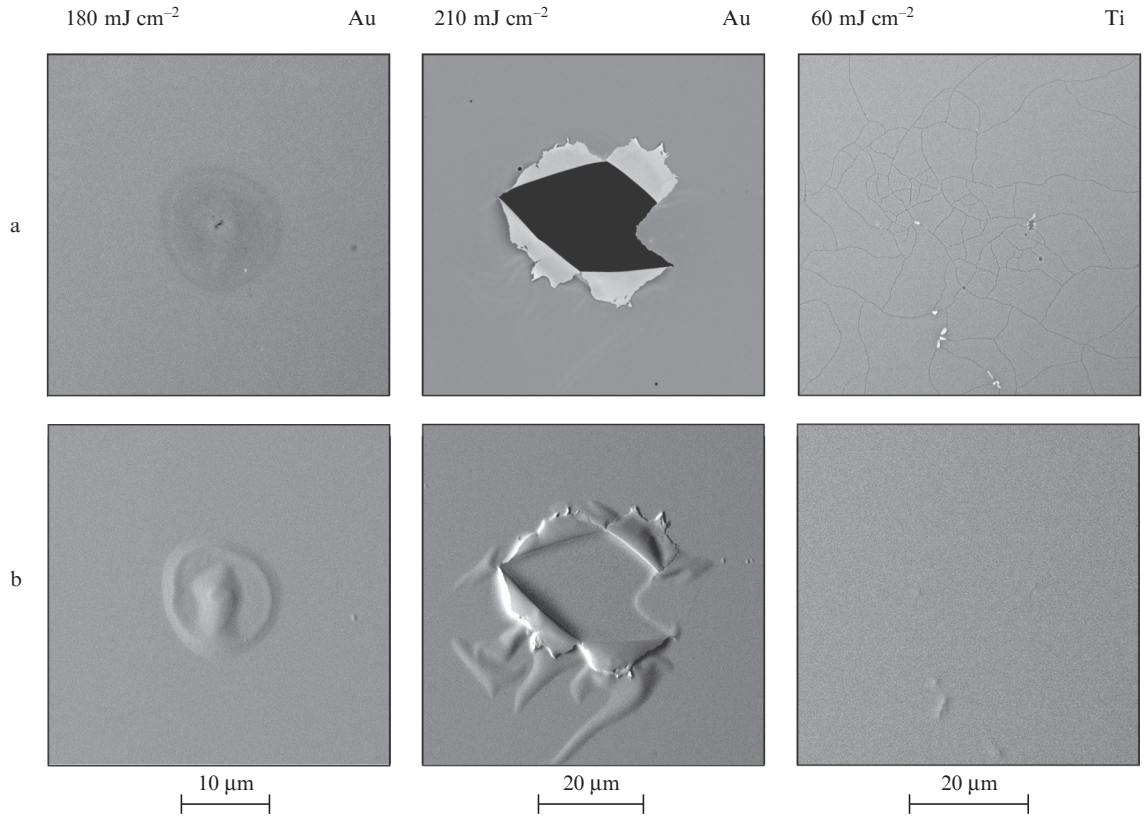

Figure 4. Images of the surfaces of gold and titanium films at the site of pulsed laser impact with fluence values close to the threshold: (a) SEM images of a metal film; (b) topographic picture of the surface.

The changes in the morphology of metal films described above, as well as their pulsed heating, lead to time-dependent changes in the film reflectivity. The dynamics of these changes determines the time dependences of the coefficients of reflection and scattering of the He–Ne laser probe beam from the metal surface and, therefore, the signal at the photodiode output (see Fig. 1).

Figure 5 shows the time dependences of the coefficient of reflection of the He–Ne laser probe beam affected by the pulsed laser impact on a gold film without gel (Fig. 5a) and with a gel layer (Fig. 5b).

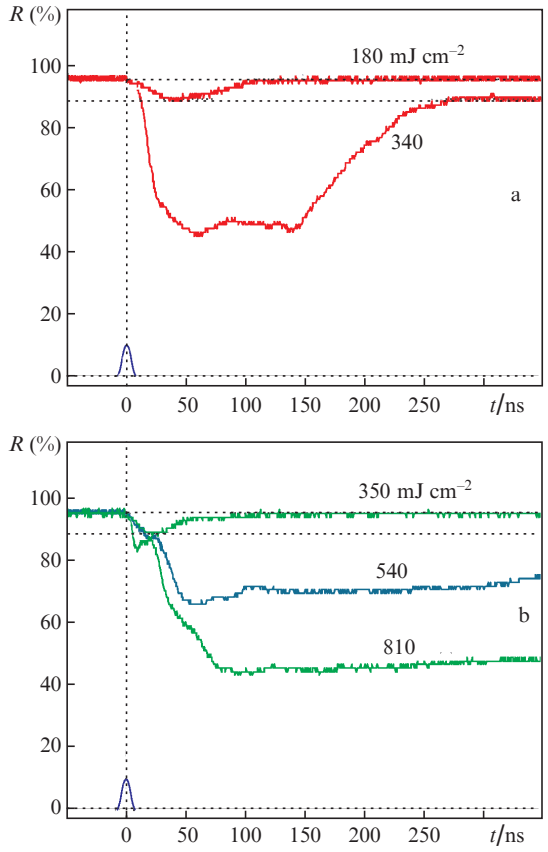

Figure 5. (Colour online) Reflectivity dynamics for the surface of the gold film on a glass substrate probed by p-polarised He–Ne laser radiation under the impact of an 8 ns laser pulse on (a) a dry metal film and (b) a film with a gel layer at various fluence values. The dashed horizontal lines correspond to the initial level of the reflected signal and a decrease in this level by 6%, and the vertical lines, to the time of reaching the maximum of the laser pulse (shown in the Figure).

Changes in the reflectivity of the Au film produced by the pulsed heating can be described based on the classical Drude theory. According to this theory, free electrons transfer the absorbed energy via collisions to the crystal lattice [24]. At a wavelength of 632.8 nm, the reflectivity decreases with increasing temperature up to the melting point of the film [19]. Therefore, the reflection coefficient measurement with a nanosecond resolution can be used to determine the onset of melting of the metal surface and to estimate the temperature at the site of pulsed impact. The character of the change in the gold film reflection coefficient at a wavelength of 632.8 nm during heating, calculated from the data of [25, 26], is shown in Fig. 6. From the dependence, it follows that upon heating

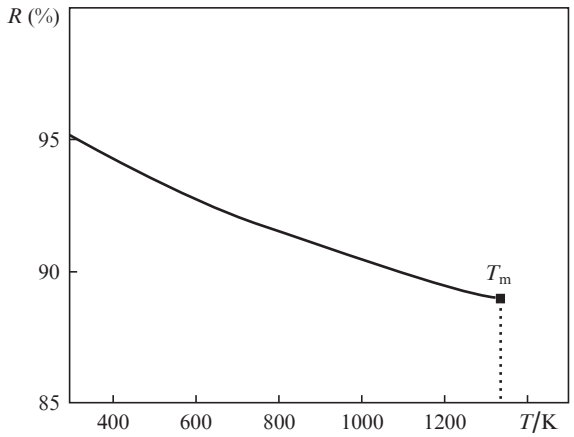

Figure 6. Dependence of the reflection coefficient of a gold film (calculated from the data of [25, 26]) for p-polarised radiation of a He–Ne laser incident at an angle of 40° on the heating temperature. The dotted line marks the melting point of gold (T_m).

a gold film to the melting point, its reflection coefficient should decrease by 6.3%.

As follows from Fig. 5, at a fluence of 180 mJ cm^{-2} in the case of a dry film and at a fluence of 350 mJ cm^{-2} in the presence of a gel, the reflected signal of the He–Ne laser after pulsed laser action decreases by about 6%, and then again reaches the initial level. According to the above calculation (see Fig. 6), the temperature of the gold film reaches the value T_m. However, the times during which the reflection coefficient $R(t)$ returns to its initial value differ little: for a film without a gel, this time is ~40 ns, and in the presence of a gel layer, about 60 ns. At a higher fluence (340 mJ cm^{-2}) in the case of a dry film (Fig. 5a), the reflection coefficient decreases to 55% in a time of ~20 ns, and T_m is reached in about 10 ns. Fluctuations in $R(t)$ are observed in the time interval 20–150 ns. Further, $R(t)$ increases monotonically and reaches a constant level, which is approximately 6% lower than the initial value. Since the gold film cooled down in a time of ~300 ns, this decrease in $R(t)$ can be explained by irreversible changes in the structure of the gold film [15].

In the case of a film with a gel layer (Fig. 5b) at a fluence of 540 mJ cm^{-2}, the slope of the initial segment of the $R(t)$ dependence corresponds to the slope at a fluence of 350 mJ cm^{-2}. In this case, the melting point is reached in the same time ~20 ns. However, in this case, $R(t)$ continues to decrease (with small fluctuations) and reaches a minimum at t = 50 ns. Then, a slight increase in $R(t)$ occurs and a plateau with a value of ~70% is observed after about 100 ns. The destruction and modification of the film that took place is probably caused by the formation of a small-diameter hole with the opening of petals and partial detachment of the film from the surface of the glass substrate (see Fig. 4).

With further increase in the fluence to 810 mJ cm^{-2} at the initial stage the rate of change in $R(t)$ increases. The melting temperature is reached as soon as in ~7 ns. Then $R(t)$ gradually decreases and after about 80 ns falls to a minimum, followed by a plateau with $R(t) \approx 45\%$. Compared to the plateau at a fluence of 540 mJ cm^{-2}, this plateau is much lower, which can be explained by the large diameter of the produced hole, as well as by more significant damage and morphological changes in the area of laser impact.

Under pulsed laser action on the surface of a titanium film, the reflection coefficient irreversibly decreases, regard-

less of the fluence value (Fig. 7). An increase in the fluence in this case leads to a decrease in the reflected signal, which is probably caused by an increase in scattering by the titanium surface due to the formation of cracks (see Fig. 4). The destruction of the dry Ti film (Fig. 7a), in comparison with the destruction of the film with the applied gel layer (Fig. 7b), occurs at a lower fluence. This result is consistent with those obtained by analysing SEM images (see Fig. 3). Note that in all cases, the time it takes for the reflected signal to reach a constant level is ~50 ns. At the same time, the obtained experimental curves for a dry surface and a surface with a gel layer did not reveal significant differences in the temporal behaviour of the signal. It can be seen from the presented examples that all these changes in the structure and morphology of the titanium film are irreversible.

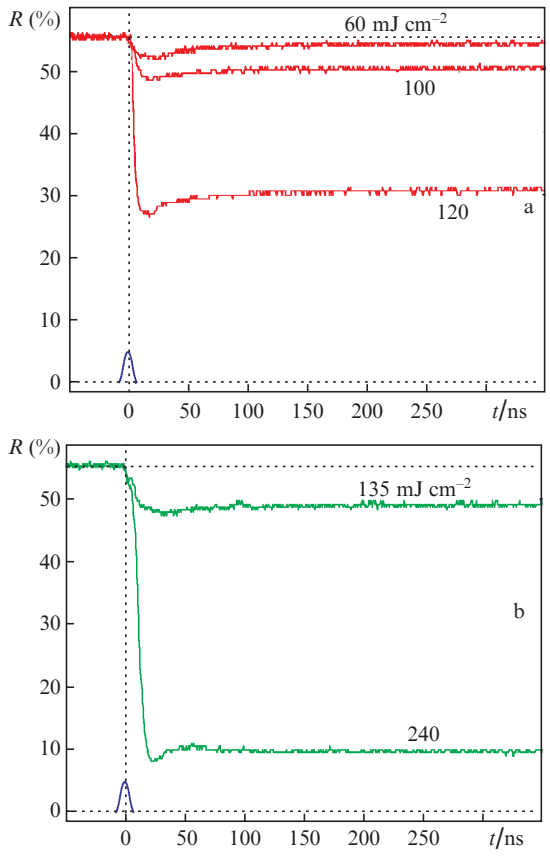

Figure 7. (Colour online) Dynamics of the reflectivity of the surface of a titanium film on a glass substrate for p-polarised radiation of a He–Ne laser under the impact of an 8 ns laser pulse on (a) a dry metal film and (b) a film with a gel layer at various values of the fluence. Dashed horizontal lines correspond to the initial level of the reflected signal, and vertical lines, to the time of reaching the maximum of the laser pulse (shown in the figure).

Unlike noble metals, titanium is a chemically active element; therefore, a titanium film is also characterised by a permanent oxide layer on its surface [27, 28]. Thus, the data of X-ray diffractometry of an intact titanium film demonstrated the presence of oxide forms of titanium in the film. Moreover, under laser irradiation of a titanium film in an aqueous solution of 2% hyaluronic acid a chemical reaction with water vapour also occurs, which can lead to the formation of nanoparticles of nonstoichiometric titanium oxide [29] and other oxide forms [30–32]. All these observations testify irreversible changes occurring in the titanium-based metal film and caused by the thermal effect of a laser pulse.

In practice, laser transfer of gel microdroplets is carried out at fluences above threshold values. Experiments have shown that pulsed laser action in this case leads to the destruction of metal absorbing films and, obviously, to the ejection of metal nanoparticles with gel microdroplets. The presence of nanoparticles in the gel substrate can adversely affect the survival of the transferred cells and microorganisms. The toxicity of gold nanoparticles was studied in [14]. A significant number of works have also been devoted to the toxicity of titanium oxides. A number of researchers point to a rather high toxic effect of titanium oxide on living cells [33, 34], others, on the contrary, did not reveal toxicity [35, 36]. At the same time, the experimental results obtained using the LEMS setup [12] showed high cell survival when using glass substrates with a titanium coating. Experimental results [37] have demonstrated that the use of glass substrates with a Ti film has a lower inhibitory effect on microorganisms as compared to a substrate with an Au film. Due to the high adhesion of the titanium film to the glass substrate, the percentage of titanium-based particles in gel microdroplets will certainly be lower than with gold-coated glass plates. Therefore, the use of titanium films in experiments on the gel transfer of living cells and microorganisms is more promising.

4. Conclusions

We studied the dynamics of morphology change and destruction of absorbing Au and Ti films of a donor substrate caused by nanosecond laser impact under conditions of gel microdroplets transfer in the range of laser fluences both above and below the ablation threshold. Experimental estimates of the threshold fluences in the case of dry films were carried out and it was shown that the presence of a gel layer on a metal film increases its ablation threshold. The time characteristics of the processes of destruction and modification of films with a nanosecond resolution were obtained from the results of measuring the intensity of the reflected He–Ne laser beam.

It was found that for a gold film, laser heating up to the melting temperature does not lead to film destruction. When the threshold fluence is slightly exceeded, a hole appears in the Au film, associated with the formation of radial ruptures and peeling of petals. For a titanium film, as a reactive metal, thermal effects near the ablation threshold are irreversible and lead to degradation of the film material with the formation of various oxide forms. Even at subthreshold fluence values, numerous cracks and micro-holes are formed in the Ti film, leading to a decrease in the reflected signal. It was shown that the presence of a gel on the film increases the ablation threshold, but the time during which the process of structural changes in the material is completed does not change significantly. The results can be used to improve the technology of laser bioprinting.

Acknowledgements. This work was partly supported by the Ministry of Science and Higher Education within the framework of the State Assignment for the Federal Research Centre 'Crystallography and Photonics' of the Russian Academy of Sciences in part of laser effects and by the Russian Science Foundation (Grant No. 20-14-00286) in part of improving the technology of microbial systems engineering.

References

1. Koch L., Kuhn S., Sorg H., Gruene M., Schlie S., Gaebel R., et al. *J. Tissue Eng. Part C: Methods*, **16** (5), 847 (2010).
2. Dinca V., Ranella A., Farsari M., Kafetzopoulos D., Dinescu M., Popescu A., Fotakis C. *Biomed. Microdevices*, **10** (5), 719 (2008).
3. Zergioti I., Karaiskou A., Papazoglou D.G., Fotakis C., Kapsetaki M., Kafetzopoulos D. *Appl. Phys. Lett*., **86** (16), 163902 (2005).
4. Yusupov V.I., Gorlenko M.V., Cheptsov V.S., Minaev N.V., Churbanova E.S., Zhigarkov V.S., et al. *Laser Phys. Lett*., **15** (6), 065604 (2018).
5. Pohl R., Visser C.W., Römer G.W., Lohse D., Sun C., Huis B. *Phys. Rev. Lett.*, **3** (2), 024001 (2015).
6. Brasz C.F., Yang J.H., Arnold C.B. *Microfluid Nanofluid*, **18** (2), 185 (2015).
7. Delaporte P., Alloncle A.P. *Opt. Laser Technol.*, **78**, 33 (2016).
8. Biver E., Rapp L., Alloncle A.P., Delaporte P. *Appl. Surf. Sci.*, **302**, 153 (2014).
9. Duocastella M., Fernández-Pradas J.M., Morenza J.L., Serra P. *J. Appl. Phys.*, **106** (8), 084907 (2009).
10. Antoshin A.A., Churbanov S.N., Minaev N.V., Deying Z., Yuanyuan Z., Shpichka A.I., Timashev P.S. *Bioprinting*, **15**, e00052 (2019). DOI: 10.1016/j.bprint.2019.e00052.
11. Yusupov V.I., Zhigarkov V.S., Churbanova E.S., Chutko E.A., Elashin S.A., Gorlenko M.V., et al. *Quantum Electron.*, **47** (12), 1158 (2017) [*Kvantovaya Elektron.*, **47** (12), 1158 (2017)].
12. Kochetkova T.V., Zayulina K.S., Zhigarkov V.S., Minaev N.V., Chichkov B.N., Novikov A.A., et al. *Int. J. Syst. Evol. Microbiol.*, **70** (2), 1192 (2020).
13. Gorlenko M.V., Chutko E.A., Churbanova E.S., Minaev N.V., Kachesov K.I., Lysak L.V., et al. *J. Biol. Eng*., **12** (1), 27 (2018).
14. Zarubin V.P., Zhigarkov V.S., Yusupov V.L., Karabutov A.A. *Quantum Electron*., **49** (11), 1068 (2019) [*Kvantovaya Elektron.*, **49** (11), 1068 (2019)].
15. Bischof J., Scherer D., Herminghaus S., Leiderer P. *Phys. Rev. Lett*., **77** (8), 1536 (1996).
16. Kuo C.C., Yeh W.C., Chen J.B., Jeng J.Y. *Thin Solid Films*, **515** (4), 1651 (2006).
17. Hatano M., Moon S., Lee M., Suzuki K., Grigoropoulos C.P. *J. Appl. Phys*., **87** (1), 36 (2000).
18. Martan J., Cibulka O., Semmar N. *Appl. Surf. Sci*., **253** (3), 1170 (2006).
19. Boneberg J., Bischof J., Leiderer P. *Opt. Commun*., **174** (1 – 4), 145 (2000).
20. Kuznetsov A.I., Koch J., Chichkov B.N. *Opt. Express*, **17** (21), 18820 (2009).
21. Low D.K.Y., Li L., Byrd P.J. *J. Manuf. Sci. Eng*., **124** (4), 852 (2002).
22. Hirano K., Fabbro R. *Phys. Procedia*, **12**, 555 (2011).
23. Jandeleit J. et al. *Appl. Phys. A*, **63** (2), 117 (1996).
24. Prokhorov A.M. et al. *Laser Heating of Metals* (Boca Raton: CRC Press, 2018).
25. Beach R.T., Christy R.W. *Phys. Rev. B*., **16** (12), 5277 (1977).
26. Reddy H. et al. *Opt. Mater. Express*, **6** (9), 2776 (2016).
27. Grigorieva T.I., Khasanov T.Kh. *Opt. Spectrosc*., **108** (4), 591 (2010) [*Opt. Spektrosk*., **108** (4), 629 (2010)].
28. Meng L.J., dos Santos M.P. *Thin Solid Films*, **226** (1), 22 (1993).
29. Simakin A.V., Voronov V.V., Shafeev G.A. *Trudy IOFAN*, **60**, 83 (2004).
30. Camacho-López S. et al. *Appl. Surf. Sci*., **255** (5), 3028 (2008).
31. Ardakani H.K. *Thin Solid Films*, **248** (2), 234 (1994).
32. Libenson M.N., Shandybina G.D., Shakhmin A.L. *Tech. Phys*., **45** (9), 1219 (2000) [*Zh. Tekh. Fiz.*, **70** (9), 124 (2000)].
33. Vamanu C.I. et al. *Toxicol. in Vitro*, **22** (7), 1689 (2008).
34. Jin C.Y. et al. *Chem. Res. Toxicol*., **21** (9), 1871 (2008).
35. Karlsson H.L. et al. *Chem. Res. Toxicol*., **21** (9), 1726 (2008).
36. Xia T. et al. *ACS Nano*, **2** (10), 2121 (2008).
37. Cheptsov V.S. et al. *Lett. Appl. Microbiol*., **67** (6), 544 (2018).